[Article] doi: 10.3866/PKU.WHXB201801091 www.whxb.pku.edu.cn

Influence of External Electric Field on Vibrational Spectrum of Imidazolium-Based Ionic Liquids Probed by Molecular Dynamics Simulation

CHEN Wenqiong [1], GUAN Yongji [1], ZHANG Xiaoping [1,*], DENG Youquan [2,*]

[1] Institute of Modern Communication, School of Information Science and Engineering, Lanzhou University, Lanzhou 730000, P. R. China.

[2] Centre for Green Chemistry and Catalysis, Lanzhou Institute of Chemical Physics, Chinese Academy Sciences, Lanzhou 730000, P. R. China.

Abstract: In this study, the influence of an external electric field (EEF) on the vibrational spectra of an imidazolium-based ionic liquid, 1-ethyl-3-methylimidazolium hexfluorophosphate ($EMIMPF_6$), in the wavenumber range from 0 to 4000 cm^{-1} was probed by molecular dynamics (MD) simulation at 350 K. The results showed that the experimentally obtained spectrum could be reproduced by the calculated vibrational bands (VBs) in the wavenumber range from 400 to 4000 cm^{-1} using MD simulation without any EEF. When the EEF applied increased from 0 to 9 $V{\cdot}nm^{-1}$, the VB intensities at 50.0 and 199.8 cm^{-1} increased continuously and then tended to be saturated, while the VB intensities from 400 to 4000 cm^{-1} decrease and eventually disappear. Moreover, the VB at 50.0 cm^{-1} was red-shifted to ~16.7 cm^{-1} and then increased to 33.3 cm^{-1} as the EEF was increased from 0 to 2 and then to 3 $V{\cdot}nm^{-1}$ and higher. The VB at 3396.6 cm^{-1} was redshifted to ~16.7 cm^{-1} and then increased to 33.3 cm^{-1} as the EEF was increased from 0 to 3 and then to 4 $V{\cdot}nm^{-1}$ and higher; however, the position of other VBs from 0 to 4000 cm^{-1} remain almost unchanged. Based on further analysis of the simulation results and previously reported studies, for the VB at 50.0 cm^{-1}, the increasing EEF enhances the polarity between cations and anions; thus, the difference in dipole moment between the cations and the anions increases, which continually increases the VB intensity until saturation is reached. For the VB at 199.8 cm^{-1}, the increasing EEF intensifies the twisting of the ethyl chain, which enhances the VB intensity until saturation. For the other VBs from 400 to 4000 cm^{-1}, the increasing EEF makes the orientation of the cations and anions in $EMIMPF_6$ more consistent; thus, it can be conjectured that such consistent orientation may weaken the VB intensities and can even make them disappear. The redshift of VB at 50.0 cm^{-1} may occur because the EEF breaks the distribution of the electrostatic field inside $EMIMPF_6$ and then weakens the interactions between cations and anions. The redshift of VB at 3396.6 cm^{-1} may be attributed to the EEF weakening the stretching vibration of the hydrogen bonds formed between the N atoms and the acidic hydrogen atoms on the cationic imidazolium rings. The EEF does not change the positions of the other VBs because the inherent stretching, bending, and rocking vibration of functional groups are not affected by the EEF.

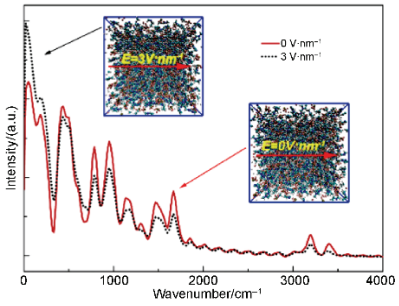

Key Words: Vibrational spectrum; External electric field; Ionic liquid; Molecular dynamics simulation

Received: December 1, 2017; Revised: January 5, 2018; Accepted: January 5, 2018; Published online: January 9, 2018.

*Corresponding authors. Email: zxp@lzu.edu.cn (Z.X.). Email: ydeng@licp.cas.cn; Tel.: +138-9366-3115 (D.Y.).

The project was supported by the National Key Research and Development Program (2017YFA0403101).
国家重点研发计划(2017YFA0403101)资助项目

分子动力学模拟研究外电场对咪唑类离子液体振动谱的影响

陈文琼[1]，关永吉[1]，张晓萍[1,*]，邓友全[2,*]

[1] 兰州大学信息科学与工程学院现代通信技术研究所，兰州 730000

[2] 中国科学院兰州化学物理研究所，绿色化学与催化研究发展中心，兰州 730000

摘要：本文利用分子动力学模拟研究了外电场对咪唑类离子液体1-乙基-3-甲基咪唑六氟磷酸盐(EMIMPF$_6$)从0到4000 cm^{-1}范围内振动谱的影响。研究结果表明，在没有外电场时利用分子动力学模拟计算得到的从400到4000 cm^{-1}的振动带可以重现实验测得的谱。当外电场从0到9 V·nm^{-1}变化时，在50.0和199.8 cm^{-1}处的振动带强度持续增强然后趋于饱和，而从400到4000 cm^{-1}的振动带强度明显减弱并最终消失。此外，在外电场从0变到2 V·nm^{-1}时，50.0 cm^{-1}的振动带红移了16.7 cm^{-1}，然后当外电场变化到3 V·nm^{-1}及更大时，该振动带红移增大到33.3 cm^{-1}。在外电场从0变到3 V·nm^{-1}时，3396.6 cm^{-1}的振动带红移大约16.7 cm^{-1},然后当外电场增大到4 V·nm^{-1}甚至更大时，该振动带红移33.3 cm^{-1},但是从0到4000 cm^{-1}的其他振动带的位置几乎没有变化。基于对模拟结果和先前报道文献的进一步分析，对于50.0 cm^{-1}的振动带，增加的外电场增强了阳离子和阴离子之间的极性使阳离子和阴离子间的偶极矩增大，因此该振动带的强度不断增大然后达到饱和。对于199.8 cm^{-1}的振动带增加的外电场增强了乙基链的扭转，使该振动带的强度增大并达到饱和。对于从400到4000 cm^{-1}的其他振动带，增加的外电场使EMIMPF$_6$ 中的阳离子和阴离子的取向更一致，并且可以推测这种更一致的取向可能会削弱振动带的强度甚至使它们消失。50.0 cm^{-1}处振动带的红移可能是由于外电场破坏了EMIMPF$_6$内部的静电场分布进而减弱了阳离子和阴离子间的相互作用。3396.6 cm^{-1}处振动带的红移可归功于外电场减弱了氮原子与阳离子咪唑环上酸性氢原子间形成的氢键的拉伸振动。对于其他的振动带，由于官能团固有的拉伸、弯曲、转动振动不受外电场的影响，外电场没有改变振动带的位置。

关键词：振动谱；外电场；离子液体；分子动力学模拟

中图分类号：O641

1 Introduction

The vibrational spectrum (VS) is produced by the transition between different vibrational energy levels in the same electron energy state in the molecule, which is located in infrared region and is also known as infrared absorption spectrum. The VS is a multi-function tool to exhibit various conformational functional groups and hydrogen bonds of both solid and liquid materials and their solutions. Earlier research work on vibrational spectra mainly focused on water using experimental [1] and computational simulation [2,3] methods. Gan and coworkers [1] used the 10 Hz and 23 ps sum frequency generation (SFG) spectrometer laser system to process the experimental measurement data and presented a detailed analysis of the SFG vibrational spectra of the air/water interface considering different polarizations and experimental configurations. Praprotnik *et al.* [3] performed a classical molecular dynamics (MD) simulation with the flexible simple point charge (SPC) and flexible extended SPC (SPC/E) water models to investigate the influence of two temperatures of −4 and 80 °C on the VS. They found that the vibrational band (VB) associated with the bending mode is consistent with the experiment, so they confirmed that the MD simulation method can successfully reproduce all other experimentally observed spectroscopic properties of bulk water. Paesani *et al.* [2] investigated hydrogen bonds dynamics in liquid water with a specific focus on the relationship of these dynamics to VS using a novel simulation approach, which combines an *ab initio*-based force field for water with a quantum treatment of the nuclear motion. The calculated spectra are in good agreement with the available experimental data, indicating the accuracy of the present simulation approach in describing the properties of liquid water under ambient conditions.

Ionic liquids (ILs) composed of bulky organic cations and organic/inorganic anions have melting points near room temperature and are known as room temperature ILs (RTILs) [4,5]. RTILs have excellent physicochemical properties such as low volatilization, high chemical and thermal stability, high ionic conductivity, a large electro-chemical potential window and remarkable solubility [6,7], which have been widely applied in lab on a chip [8], variable-focus lenses [9], flow-induced energy harvesting [10,11], electro-wetting [12,13] in recent years. RTILs have attracted much theoretical interest for broad applications as environmentally friendly solvents in chemical and industrial processes, so a better understanding of physicochemical properties and structures of bulk pure RTILs is critically important for the vast majority of these applications. Jeon *et al.* [14] experimentally investigated the structures of ILs 1-butyl-3-methylimidazolium iodide, BMIMI and 1-butyl-3-methylimidazolium tetrafluoroborate, BMIMBF$_4$ and their aqueous mixtures from the attenuated total reflection (ATR)

infrared absorption spectra. They found that the infrared absorption spectrum of cation $BMIM^+$ is very different in these two ILs and changes with increase of the water concentration due to the difference of the relative position between the anions and cations. Bhargava and Balasubramanian [15] studied the VS of imidazolium based IL 1,3-dimethylimidazolium chloride, MMIMCl which was calculated by the Fourier transform of the normalized velocity autocorrelation function (VACF) of all atoms obtained from the trajectory in the system using Car-Parrinello MD simulation (CPMD). They found that the results were in good agreement with spectroscopic data in the experiment, which indicated the hydrogen bond between the acidic hydrogen atom on the cationic imidazolium rings and the chloride ion could be obtained not only through structural data but also through vibrational dynamics of the cation and the latter was more direct comparing with experimental method. Katsyuba *et al.* [16] investigated possible molecular structure of the ion pairs in several imidazolium based ILs (halides, tetrafluoroborates, and hexafluorophosphate based imidazolium salts) using density functional theory (DFT) method in combination with VS, and meanwhile revealed both common features and differences in structure of various imidazolium based ILs. They also found that vibrations of cations not only depend on the conformational changes but also on the association with counterions on the basis of previous research.

As we all known, electric fields are significant to analyze the regulating macroscopic and microscopic properties of ILs. Ricks-Laskoski and Snow [17] pointed out that polymerizable ILs and their actuation in an electric field are combination of material and properties with unique potential to display structural and fluid dynamics above that found for small molecule ILs. However, there have few reports focused on the influence of the external electric field (EEF) on the VS for ILs using MD simulation method. Comparing with the DFT method, MD simulation method can study the VS for ILs systems containing more cation and anion pairs on the nanoscale. Under these circumstances, the VS for larger ILs systems under EEF need to be investigated using MD simulation method. In this study, we performed a classical MD simulation to investigate the influence of the EEF varied from 0 to 9 $V{\cdot}nm^{-1}$ on the VS of imidazolium-based IL 1-ethyl-3-methylimidazolium hexfluorophosphate, $EMIMPF_6$ system consisting of 512 ILs pairs in the range from 0 to 4000 cm^{-1}. The VS envelope was calculated by a Fourier transform of the normalized VACF. Firstly, we calculated the VS of $EMIMPF_6$ in the range from 0 to 4000 cm^{-1} and found the main features of the experimentally measured spectrum are reproduced by the calculated VBs using MD simulation. Secondly, the VS of $EMIMPF_6$ in the range from 0 to 4000 cm^{-1} was calculated by a Fourier transform of the normalized VACF of all atoms obtained from the trajectory in the system under an EEF of 3 $V{\cdot}nm^{-1}$. Finally, the influence of EEF strength on the intensities and position of VS was also investigated. In particular, we found the EEF not only changes the intensities of the VS but also changes the position of the VS that make the VS show a redshift.

2 Computational methods

2.1 Molecular models

In this study, the imidazolium based IL $EMIMPF_6$ is employed to probe the VS under the action of the EEF varied from 0 to 9 $V{\cdot}nm^{-1}$ using MD simulation, and the molecular structures of the cation and anion used are showed in Fig. 1. The initial cube model of $EMIMPF_6$ with dimensions of 5.16 × 5.16 × 5.16 nm constructed by PACKMOL software [18], where the initial structure of the single IL pairs is derived from the Cambridge Crystallographic Data Centre (CCDC). Periodic boundary conditions (PBC) are applied to all directions of the simulated box in the whole MD simulation. Fig. 2 shows the ensemble structure with the initial cube model including 512 $EMIMPF_6$ ion pairs obtained from a separate MD simulation, which is visualized with a molecular graphics software named visual molecular dynamics (VMD) [19].

2.2 Simulation details

All MD simulations were carried out using the general purpose parallel MD simulation open-source package DL_POLY 4.08 [20]. The non-polarizable force field of ILs employed is based on the systematic all-atom force fields (AA-FFs) developed by the work of Canongia Lopes and Padua [21] that is in the frame of optimized potential for liquid simulation/all atom (OPLS-AA) force field [22,23], which is a combination of parameters derived from quantum chemical calculations and force fields published in the literature. Its potential energy's functional expression is

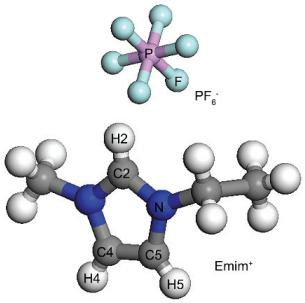

Fig. 1 The molecular structures of 1-ethyl-3-methylimidazolium ($EMIM^+$) and hexafluorophosphate (PF_6^-).

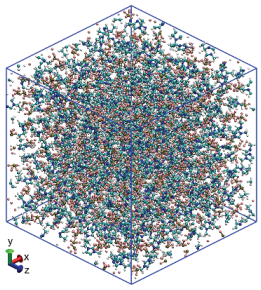

Fig. 2 Initial structure of the ensemble.

$$U_{\text{total}} = U_{\text{bonds}} + U_{\text{angles}} + U_{\text{dihedrals}} + U_{\text{vdw}} + U_{\text{coul}}$$
$$= \sum_{\text{bond}} \frac{1}{2} k_{\text{r}} (r - r_0)^2 + \sum_{\text{angles}} \frac{1}{2} k_\theta (\theta - \theta_0)^2 +$$
$$\sum_{\text{dihedrals}} V_n \left[1 + \cos\left(n\varphi - \gamma\right)\right] + \quad (1)$$
$$\sum_i \sum_{j>i} 4\varepsilon \left[\left(\frac{\sigma}{r_{ij}}\right)^{12} - \left(\frac{\sigma}{r_{ij}}\right)^{6}\right] + \sum_i \sum_{j>i} \frac{1}{4\pi\varepsilon} \frac{q_i q_j}{r_{ij}}$$

where the total energy of the given system is the sum of bond stretch, bond angle bend, dihedral torsion, and pairwise nonbonding energies concluding the van der Waals (VDW) interactions computed by the Lorentz-Berthelot combining rules, and Coulombic interaction of partial atomic charges.

In the MD simulation process, the Newton's motion equations were integrated by using a velocity verlet algorithm with an integration timestep of 2.0 fs. The initial velocities were assigned to the atoms randomly according to the system's temperature. Long range Coulombic interactions were treated using the smooth particle mesh Ewald (PME) method [24]. The VDW and the real space electrostatic interactions were truncated and shifted to zero at 1.5 nm.

The MD simulation of $EMIMPF_6$ was employed with the system consisting of 512 ion pairs, and was performed using the Nosé-Hoover thermostat [25,26]. The thermostat was set to the temperature according to the melting point of $EMIMPF_6$ in the system. The initial configuration was then equilibrated with a NPT ensemble for $p = 1.01325 \times 10^5$ Pa and $T = 350$ K until the experimental value of the liquid density was achieved and the total energy of the system converged to a constant after 10 ns with time step of 2.0 fs (Fig. S1). Then the obtained equilibrated configuration at $T = 350$ K was allowed to run for another 10ns with a NVT ensemble to ensure a better equilibrium state. Finally, a sample procedure was taken every 1000 time steps for $EMIMPF_6$ configuration to obtain the statistically equilibrium averaged values in the next 10 ns.

2.3 Calculation of VS

The VS could be used to study structures and hydrogen bonds of ILs, and there are usually two methods to calculate the VS, which are the Fourier transforming of the system's total dipole moment autocorrelation function and the Fourier transforming of the VACF [3]. In this paper, we calculate the VS using the second method. The VS is obtained by the Fourier transforming of the VACF as

$$I(\omega) \propto \int_0^\infty \left\langle C_\upsilon(t) \cdot C_\upsilon(0) \right\rangle \mathrm{e}^{-\mathrm{j}\omega t} \mathrm{d}t \quad (2)$$

where $I(\omega)$ is the VS intensity, $C_\upsilon(t)$ is the centroid equivalence of the normalized VACFs of all atoms in the system at time t, ω is the VS frequency, and the angular bracket represents an average taken over all time origins. The normalized VACF of the single ion at time t is calculated by

$$C_\upsilon(t) = \frac{\left\langle \upsilon_{\text{c}}(t) \cdot \upsilon_{\text{c}}(0) \right\rangle}{\left\langle \upsilon_{\text{c}}(0) \cdot \upsilon_{\text{c}}(0) \right\rangle} \quad (3)$$

where $\upsilon_{\text{c}}(t)$ is the velocity of the center of mass of the single ion in the system at time t. In strongly coupled molecular systems with a large number of atoms, the VACFs of all atoms should fluctuate and decay to zero very rapidly within a small number of vibrational periods about 2 ps.

3 Results and discussion

3.1 Without EEF

After the system reaches equilibration, the VS of imidazolium-based IL $EMIMPF_6$ is calculated by the Fourier transforming of the normalized VACFs of all atoms in the system. The VS for the pure $EMIMPF_6$ in the range from 0 to 4000 cm^{-1} are showed in Fig. 3. It is clearly seen that the main features of the experimentally measured spectrum are reproduced by the calculated VBs using MD simulation (Fig. S2). Through comparing with the VS obtained from experiments [27] and DFT calculation [16], we found the VS in Fig. 3 which obtains from the MD simulation is reasonable and receivable. It is worth noting that the numbers of the VBs obtained using MD simulation are obviously less than the VBs measured in experiments, this because the $EMIMPF_6$ used in experiment is not completely pure IL and includes some impurities which can generate some noise peaks. Therefore, the VS obtained from MD simulation may more accurately reflect the real situation.

The VBs wavenumbers and assignments for $EMIMPF_6$ are listed in Table 1. As showed in Table 1, the calculated vibrations assigned to these bands including C—H in the imidazolium ring stretching mode (3196.8 cm^{-1}), the ring C=C stretching mode (1620.7 cm^{-1}), the terminal CH_3 anti-symmetrical H—C—H bending mode (1465.2 cm^{-1}), the terminal CH_3 rocking mode (1132.2 cm^{-1}), the ethyl side chain C—C stretching mode (949.0 cm^{-1}), the ethyl side chain CH_2 and CH_3 rocking modes (782.6 cm^{-1}), the N atom in the imidazolium ring and the ethyl side chain/terminal CH_3 rocking modes (432.9 cm^{-1}), and the torsion of the ethyl side chain (199.8 cm^{-1}). Particularly, there are two VBs at 50.0 cm^{-1} assigned to the cations and anions torsion [28–30] belonging to far-infrared region and 3396.6 cm^{-1} assigned to the

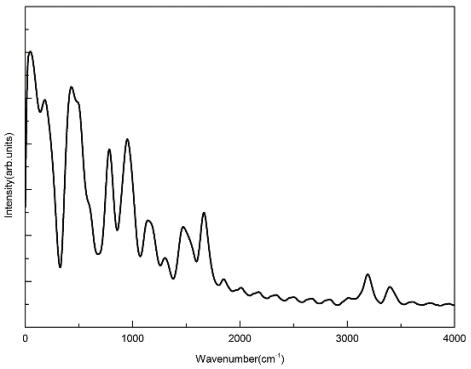

Fig. 3 The VS (arbitrary units) of $EMIMPF_6$ calculated by Fourier transforming of all atoms' VACFs without EEF.

Table 1 VS of $EMIMPF_6$ without EEF.

Wavenumber (cm^{-1}) [a]	Assignment [b]
50.0 vvs	Cat-An tors
199.8 m	tors Et
432.9 vvs br	r N-Et, r N-Me
782.6 s	r CH_2, r CH_3 (Et)
949.0 s	ν CC (Et)
1132.2 m sh	r CH_3
1465.2 m	δ_{as} CH_3
1620.7 m	ν C=C
3196.8 m	ν C2−H2
	ν C4−H4, C5−H5
3396.6 m	ν N−H2

[a] Labels: m, medium; s, strong; v, very; sh, shoulder; br, broad.

[b] Labels: ν, stretch; δ, bend; r, rocking; Et, ethyl; Me, methyl.

intermolecular hydrogen bonds formed by N atoms and acidic H atoms on the cationic imidazolium rings. The VB at 50.0 cm^{-1} can be attributed to the intermolecular interaction between cations and anions, which provides a new method to probe the cation-anion interaction in ILs by far-infrared spectrum [30]. To illustrate the association of the intermolecular hydrogen bonds, we calculate the radial distribution functions (RDFs) of the N atom and H2/H4/H5 atoms in the imidazolium ring. The RDFs for the N atom and the H atom in the imidazolium ring are showed in Fig. 4, which describes the probability of finding the selected atomic site around others in the system. From Fig. 4, we can get that the electrostatic interaction between N atom and H2 atom is stronger than between N atom and H4/H5 atom. The higher intensity of distribution between N atom and H2 atom in Fig. 4 indicates the intermolecular hydrogen bonds consisting of N atom and H2 atom in the imidazolium ring. To further illustrate the intermolecular hydrogen bonds between N atoms and H2 atoms, we calculate the average numbers of H2 atoms around N atoms in the radius of 0.3 nm and find that there are two H2 atoms around N atoms (Fig. S3). This can confirm the intermolecular hydrogen bonds are formed between N atoms and adjacent H2 atoms in different cations.

3.2 EEF

The VS of $EMIMPF_6$ under an EEF of 3 $V{\cdot}nm^{-1}$ in the range between 0 to 4000 cm^{-1} are presented in Fig. 5. As showed in Fig. 5, the relative intensities of VBs at 50 cm^{-1} and 200 cm^{-1} significantly enhance under an EEF, while the VB intensities from 400 cm^{-1} to 4000 cm^{-1} obviously weaken under an EEF. On the other hand, the VBs at 50.0 cm^{-1} and 3396.6 cm^{-1} redshift about 33 and 16 wavenumbers respectively and the positions of other VBs are almost unchanged.

It is well known that the VBs intensities below 200 cm^{-1} in the far-infrared region represent the interaction strength between cations and anions [30], while the VBs between 400 cm^{-1} and 4000 cm^{-1} represent the vibrational characteristic of functional groups including groups on cationic imidazolium ring and ethyl/methyl side chains, and so on. Fig. 5 clearly shows that the VB intensities at 50.0 cm^{-1} and 199.8 cm^{-1} between cations and anions enhance under an EEF of 3 $V{\cdot}nm^{-1}$. In the case of the VB at 50.0 cm^{-1}, the EEF makes the distance between cations and anions increase (from 0.528 to 0.534 nm) that enhances the polarity between cations and anions and thus the change of the dipole moment between the cations and the anions grows up. The increase of the change of the dipole moment makes the VB intensity at 50.0 cm^{-1} enhance. In the case of VB at 199.8 cm^{-1}, the EEF intensifies the twisting of the ethyl chain, which enhances the VB intensity at 199.8 cm^{-1}. This is confirmed by the calculated the orientation of the ethyl chain in Fig. 6. From Fig. 6, we can find the values of second Legendre polynomials ($P_2(\cos(\theta)) = (3\cos^2(\theta) - 1)/2$) about the orientation angle significantly increase under an EEF of 3 $V{\cdot}nm^{-1}$ comparing with the values without EEF. This indicates the twisting of the ethyl chain enhances indeed and so enhances the VB intensity at 199.8 cm^{-1}. For other VBs from 400 cm^{-1} to 4000 cm^{-1}, the EEF changes the distribution structures of cations and anions and make them rearrange, thus the orientation of the cations and anions in $EMIMPF_6$ is more consistent (Fig. 6) and we conjectured this consistent orientation maybe weaken the VB intensities.

As showed in Fig. 5, the EEF not only changes the VS intensities but also changes the VS position. Under an EEF of 3 $V{\cdot}nm^{-1}$, the VB at 50.0 cm^{-1} redshifts about 33.3 wavenumbers. This redshift of VB at 50.0 cm^{-1} is mainly

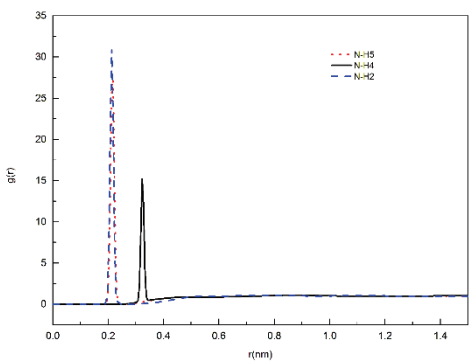

Fig. 4 RDFs between nitrogen atom connecting the ethyl side chain and hydrogen atoms on the cationic imidazolium rings without EEF.

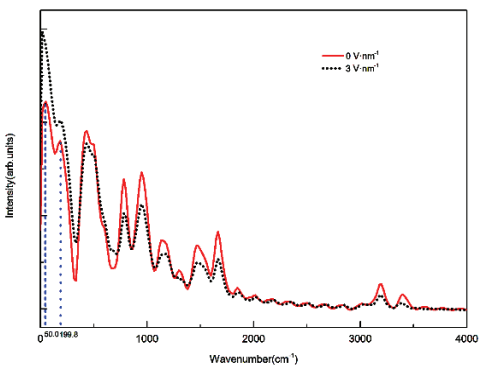

Fig. 5 The vibrational spectra (arbitrary units) of $EMIMPF_6$ under an EEF of 0 and 3 $V{\cdot}nm^{-1}$.

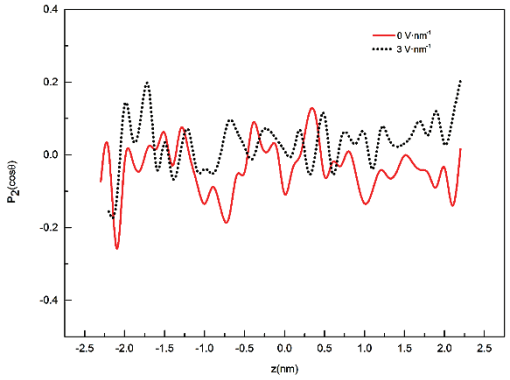

Fig. 6 Average values of $P_2(\cos(\theta))$ for the angles between the selected vector (N atom and thermal C atom on the ethyl side chain) and the vector that is perpendicular to the direction of EEF (z axis) in the system under EEF of 0 and 3 V·nm^{-1}.

caused by the EEF breaks the distribution of the electrostatic field inside $EMIMPF_6$ and then weakens interactions between cations and anions. In order to more intuitively explain the weakening of the interactions between cations and anions, the RDFs of cations and anions are calculated and presented in Fig. 7. It can be visually seen from Fig. 7 that the first peak value of RDFs under an EEF of 3 V·nm^{-1} is less than the first peak value of RDFs without EEF. This indicates the interactions between cations and anions weaken under an EEF and thus the VB at 50.0 cm^{-1} shows a redshift. Likewise, the VB at 3396.6 cm^{-1} redshifts about 16.7 wavenumbers under an EEF of 3 V·nm^{-1}. This redshift may be attributed to the EEF weakens the stretching vibration of hydrogen bonds formed by N atoms and acidic H atoms on the cationic imidazolium rings. The stretching vibration of hydrogen bonds weakening can be confirmed in results reported in Fig. 8. The first peak value of RDFs under an EEF of 3 V·nm^{-1} is higher than the first peak value without EEF, which indicates the numbers of H atoms around N atoms increase, this can be confirmed by the calculated average numbers of H atoms around N atom which varies from 1.95 to 1.98 in the radius of 0.22 nm. Thus, the probability to form hydrogen bonds increases and more hydrogen bonds generate. Therefore, the stretching vibration of hydrogen bonds enhances and the VB at 3396.6 cm^{-1} shows a redshift. For other VBs from 0 to 4000 cm^{-1}, the EEF does not change the positions of VBs due to the inherent stretching, bending and rocking vibration of functional groups are not affected by the EEF.

Additionally, the influence of EEF strength on the VS of $EMIMPF_6$ was also investigated in the range from 0 to 4000 cm^{-1}. The MD simulations performed with different EEF varied from 0 to 9 V·nm^{-1} would allow for interference of the effect of EEF on the VS of $EMIMPF_6$. Though applying different EEF on the $EMIMPF_6$, we found the VB intensities at 50.0 cm^{-1} and 199.8 cm^{-1} continually enhanced and then tended to be saturated, while the VB intensities from 400 cm^{-1} to 4000 cm^{-1} obviously weakened and eventually disappeared with increase of EEF strength (Fig. S4). The VS of $EMIMPF_6$ under the EEF varied from 0 to 4 V·nm^{-1} were showed in Fig. 9. For the VB at 50.0 cm^{-1}, the increasing EEF enhances the polarity between cations and anions and thus the change of the dipole moment between the cations and the anions grows up, which makes the VB intensity continually enhance and then reach saturation. For the VB at 199.8 cm^{-1}, the increasing EEF intensifies the twisting of the ethyl chain, which makes the VB intensity increase to be saturated. For other VBs from 400 to 4000 cm^{-1}, the increasing EEF makes the orientation of the cations and anions in $EMIMPF_6$ more and more consistent and we conjectured this consistent orientation maybe weaken the

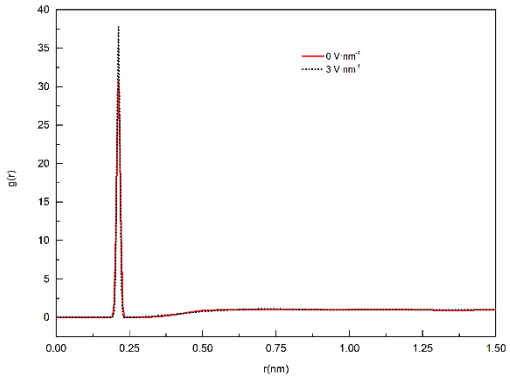

Fig. 8 RDFs between N atom connecting the ethyl side chain and H atoms on the cationic imidazolium rings under EEF of 0 and 3 V·nm^{-1}.

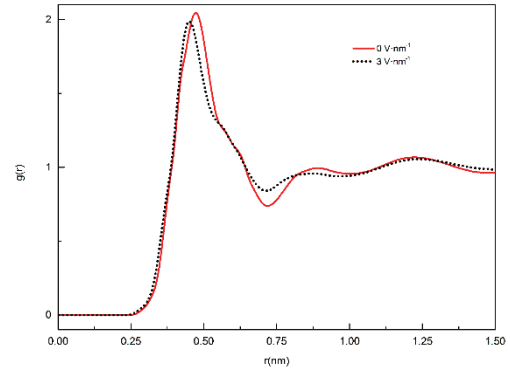

Fig. 7 RDFs of cations and anions in $EMIMPF_6$ under EEF of 0 and 3 V·nm^{-1}.

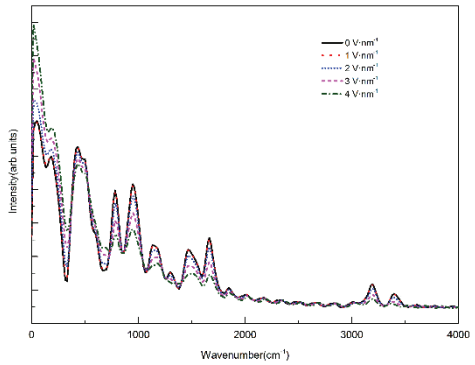

Fig. 9 The vibrational spectra (arbitrary units) of $EMIMPF_6$ under different EEF.

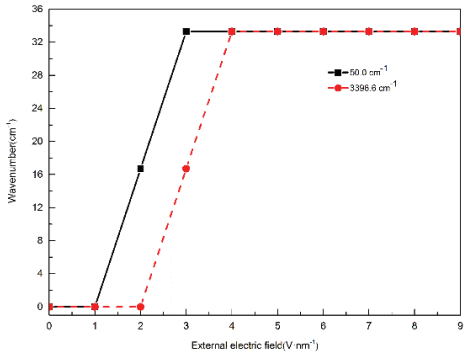

Fig. 10 The redshift of VBs at 50.0 and 3396.6 cm^{-1} under different EEF.

VB intensities and even make them disappear. Moreover, as showed in Fig. 10, the VBs at 50.0 cm^{-1} redshifted about 16.7 cm^{-1} as the EEF varied from 0 to 2 V·nm^{-1} and the redshift increased to 33.3 cm^{-1} as the EEF varied from 2 to 3 V·nm^{-1} and further > 3 V·nm^{-1}. The VBs at 3396.6 cm^{-1} redshifted about 16.7 cm^{-1} under the EEF varied from 0 to 3 V·nm^{-1} and the redshift increased to 33.3 cm^{-1} as the EEF varied from 3 to 4 V·nm^{-1} and further > 4 V·nm^{-1}, but the position of other VBs from 0 to 4000 cm^{-1} are almost unchanged. The redshift of VB at 50.0 cm^{-1} from 16.7 to 33.3 cm^{-1} may be caused by the increasing EEF first breaks the distribution of the electrostatic field inside EMIMPF$_6$ and eventually keep balance with the inner electrostatic field. The redshift of VB at 3396.6 cm^{-1} is not entirely clear and this result may be attributed to the increasing EEF weakens the stretching vibration of hydrogen bonds formed by N atoms and the acidic hydrogen atoms on the cationic imidazolium rings and finally the stretching vibration is almost unchanged. For other VBs, the EEF does not change the positions of VBs due to the inherent stretching, bending and rocking vibration of functional groups are not affected by the EEF.

4 Conclusions

In summary, here we investigate the influence of EEF on the vibrational spectra of imidazolium-based IL EMIMPF$_6$ in the range from 0 to 4000 cm^{-1} using classical MD simulation. The research results showed that the experimentally measured spectrum could be reproduced by the calculated VBs in the range from 400 to 4000 cm^{-1} using MD simulation without such EEF. Under the EEF ranging from 0 to 9 V·nm^{-1}, the VB intensities at 50.0 and 199.8 cm^{-1} continually enhance then tend to be saturated, while the VB intensities from 400 to 4000 cm^{-1} obviously weaken and eventually disappear. Moreover, the VB at 50.0 cm^{-1} redshifted about 16.7 then increased to 33.3 cm^{-1} as the EEF varied from 0 to 2 then to 3 V·nm^{-1} and further. The VB at 3396.6 cm^{-1} redshifted about 16.7 then increased to 33.3 cm^{-1} as the EEF varied from 0 to 3 then to 4 V·nm^{-1} and further, but the position of other VBs from 0 to 4000 cm^{-1} are almost unchanged. Based on further analysis on the simulation results and previous reported literatures, for the VB at 50.0 cm^{-1}, the increasing EEF enhances the polarity between cations and anions and thus the change of the dipole moment between the cations and the anions grows up, which makes the VB intensity continually enhance and then reach saturation. For the VB at 199.8 cm^{-1}, the increasing EEF intensifies the twisting of the ethyl chain, which makes the VB intensity increase to be saturated. For other VBs from 400 to 4000 cm^{-1}, the increasing EEF makes the orientation of the cations and anions in EMIMPF$_6$ more consistent and it can be conjectured that such more consistent orientation may weaken the VB intensities and even make them disappear. The redshift of VB at 50.0 cm^{-1} may be caused by the EEF breaks the distribution of the electrostatic field inside EMIMPF$_6$ and then weakens interactions between cations and anions. The redshift of VB at 3396.6 cm^{-1} may be attributed to the EEF weakens the stretching vibration of hydrogen bonds formed by N atoms and the acidic hydrogen atoms on the cationic imidazolium rings. For other VBs, the EEF does not change the positions of VBs due to the inherent stretching, bending and rocking vibration of functional groups are not affected by the EEF. These results may be significant for opening prospects to investigate the effect of external field on properties of ILs.

Supporting Information: available free of charge *via* the internet at http://www.whxb.pku.edu.cn.

References

(1) Gan, W.; Wu, D.; Zhang, Z.; Feng, R. R.; Wang, H. F. *J. Chem. Phys.* **2006,** *124*, 114705. doi: 10.1063/1.2179794

(2) Paesani, F.; Xantheas, S. S.; Voth, G. A. *J. Phys. Chem. B* **2009,** *113*, 13118. doi: 10.1021/jp907648y

(3) Praprotnik, M.; Janežič, D.; Mavri, J. *J. Phys. Chem. A* **2004,** *108*, 11056. doi: 10.1021/jp046158d

(4) Austen Angell, C.; Ansari, Y.; Zhao, Z. *Faraday Discuss.* **2012,** *154*, 9. doi: 10.1039/c1fd00112d

(5) Ott, L. S.; Cline, M. L.; Deetlefs, M.; Seddon, K. R.; Finke, R. G. *J. Am. Chem. Soc.* **2005,** *127*, 5758. doi: 10.1021/ja0423320

(6) Plechkova, N. V.; Seddon, K. R. *Chem. Soc. Rev.* **2008,** *37*, 123. doi: 10.1039/b006677j

(7) Zhang, S. G.; Zhang, J. H.; Zhang, Y.; Deng, Y. Q. *Chem. Rev.* **2017,** *117*, 6755. doi: 10.1021/acs.chemrev.6b00509

(8) He, X. D.; Shao, Q. F.; Cao, P. F.; Kong, W. J.; Sun, J. Q.; Zhang, X. P.; Deng, Y. Q. *Lab Chip* **2015,** *15*, 1311. doi: 10.1039/c4lc01434k

(9) Hu, X. D.; Zhang, S. G.; Qu, C.; Zhang, Q. H.; Lu, L. J.; Ma, X. Y.; Zhang, X. P.; Deng, Y. Q. *Soft Matter* **2011,** *7*, 5941. doi: 10.1039/c1sm05585b

(10) Kong, W. J.; Cheng, L.; He, X. D.; Xu, Z. H.; Ma, X. Y.; He, Y. D.; Lu, L. J.; Zhang, X. P.; Deng, Y. Q. *Microfluid. Nanofluid.* **2014,**

18, 1299. doi: 10.1007/s10404-014-1528-2

(11) Shao, Q. F.; Jia, J. J.; Guan, Y. J.; He, X. D.; Zhang, X. P. *J. Chem. Phys.* **2016,** *144*, 124703. doi: 10.1063/1.4944611

(12) Guan, Y. J.; Shao, Q. F.; Chen, W. Q.; Liu, S. M.; Zhang, X. P.; Deng, Y. Q. *J. Phys. Chem. C* **2017,** *121*, 23716. doi: 10.1021/acs.jpcc.7b07474

(13) Hu, X. D.; Zhang, S. G.; Liu, Y.; Qu, C.; Lu, L. J.; Ma, X. Y.; Zhang, X. P.; Deng, Y. Q. *Appl. Phys. Lett.* **2011,** *99*, 213505. doi: 10.1063/1.3663633

(14) Jeon, Y.; Sung, J.; Seo, C.; Lim, H.; Cheong, H.; Kang, M.; Moon, B.; Ouchi, Y.; Kim, D. *J. Phys. Chem. B* **2008,** *112*, 4735. doi: 10.1021/jp7120752

(15) Bhargava, B. L.; Balasubramanian, S. *Chem. Phys. Lett.* **2006,** *417*, 486. doi: 10.1016/j.cplett.2005.10.050

(16) Katsyuba, S. A.; Zvereva, E. E.; Vidis, A.; Dyson, P. J. *J. Phys. Chem. A* **2007,** *111*, 352. doi: 10.1021/jp064610i

(17) Ricks-Laskoski, H. L.; Snow, A. W. *J. Am. Chem. Soc.* **2006,** *128*, 12402. doi: 10.1021/ja064264i

(18) Martinez, L.; Andrade, R.; Birgin, E. G.; Martinez, J. M. *J. Comput. Chem.* **2009,** *30*, 2157. doi: 10.1002/jcc.21224

(19) Humphrey, W.; Dalke, A.; Schulten, K. *J. Mol. Graphics* **1996,** *14*, 33. doi: 10.1016/0263-7855(96)00018-5

(20) Todorov, I. T.; Smith, W.; Trachenko, K.; Dove, M. T. *J. Mater. Chem.* **2006,** *16*, 1911. doi: 10.1039/b517931a

(21) Lopes, J. N. C.; Pádua, A. l. A. H. *J. Phys. Chem. B* **2004,** *108*, 16893. doi: 10.1021/jp0476545

(22) Jorgensen, W. L.; Maxwell, D. S.; Tirado-Rives, J. *J. Am. Chem. Soc.* **1996,** *118*, 11225. doi: 10.1021/ja9621760

(23) Kaminski, G.; Jorgensen, W. L. *J. Phys. Chem.* **1996,** *100*, 18010. doi: 10.1021/jp9624257

(24) Essmann, U.; Perera, L.; Berkowitz, M. L.; Darden, T.; Lee, H.; Pedersen, L. G. *J. Chem. Phys.* **1995,** *103*, 8577. doi: 10.1063/1.470117

(25) Hoover, W. G. *Phys. Rev. A* **1985,** *31*, 1695. doi: 10.1103/PhysRevA.31.1695

(26) Nosé, S. *J. Chem. Phys.* **1984,** *81*, 511. doi: 10.1063/1.447334

(27) Heimer, N. E.; Del Sesto, R. E.; Meng, Z.; Wilkes, J. S.; Carper, W. R. *J. Mol. Liq.* **2006,** *124*, 84. doi: 10.1016/j.molliq.2005.08.004

(28) Talaty, E. R.; Raja, S.; Storhaug, V. J.; Do1lle, A.; Carper, W. R. *J. Phys. Chem. B* **2004,** *108*, 13177. doi: 10.1021/jp040199s

(29) Fumino, K.; Wittler, K.; Ludwig, R. *J. Phys. Chem. B* **2012,** *116*, 9507. doi: 10.1021/jp306173t

(30) Fumino, K.; Wulf, A.; Ludwig, R. *Angew. Chem. Int. Ed.* **2008,** *47*, 3830. doi: 10.1002/anie.200705736